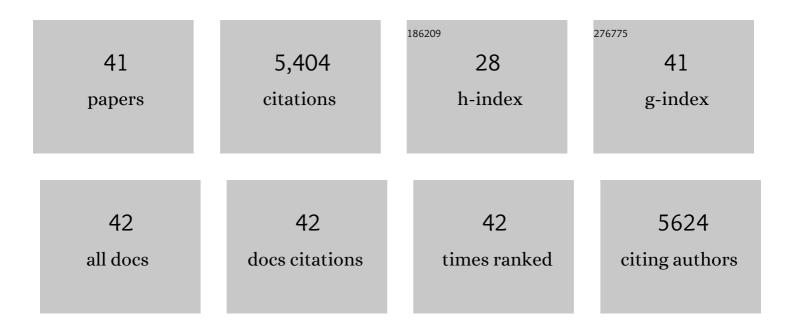
Allan Balmain

List of Publications by Year in descending order

Source: https://exaly.com/author-pdf/741451/publications.pdf Version: 2024-02-01



Διιών Βλιμαίν

#	Article	IF	CITATIONS
1	Carcinogen-specific mutation and amplification of Ha-ras during mouse skin carcinogenesis. Nature, 1986, 322, 78-80.	13.7	846
2	Activation of the mouse cellular Harvey-ras gene in chemically induced benign skin papillomas. Nature, 1984, 307, 658-660.	13.7	550
3	Mouse skin carcinomas induced in vivo by chemical carcinogens have a transforming Harvey-ras oncogene. Nature, 1983, 303, 72-74.	13.7	427
4	Metastasis is driven by sequential elevation of H-ras and Smad2 levels. Nature Cell Biology, 2002, 4, 487-494.	4.6	348
5	p53-deficient mice are extremely susceptible to radiation-induced tumorigenesis. Nature Genetics, 1994, 8, 66-69.	9.4	347
6	The mutational landscapes of genetic and chemical models of Kras-driven lung cancer. Nature, 2015, 517, 489-492.	13.7	285
7	A model for RAS mutation patterns in cancers: finding the sweet spot. Nature Reviews Cancer, 2018, 18, 767-777.	12.8	266
8	Skin hyperkeratosis and papilloma formation in transgenic mice expressing a ras oncogene from a suprabasal keratin promoter. Cell, 1990, 62, 697-708.	13.5	265
9	Stem-cell hierarchy in skin cancer. Nature Reviews Cancer, 2003, 3, 434-443.	12.8	261
10	K-Ras Promotes Tumorigenicity through Suppression of Non-canonical Wnt Signaling. Cell, 2015, 163, 1237-1251.	13.5	195
11	The malignant capacity of skin tumours induced by expression of a mutant H-ras transgene depends on the cell type targeted. Current Biology, 1998, 8, 516-524.	1.8	143
12	Cancer as a Complex Genetic Trait. Cell, 2002, 108, 145-152.	13.5	131
13	Distinct genetic loci control development of benign and malignant skin tumours in mice. Nature Genetics, 1995, 10, 424-429.	9.4	120
14	Genetic architecture of mouse skin inflammation and tumour susceptibility. Nature, 2009, 458, 505-508.	13.7	120
15	Kras regulatory elements and exon 4A determine mutation specificity in lung cancer. Nature Genetics, 2008, 40, 1240-1244.	9.4	113
16	Evolution of metastasis revealed by mutational landscapes of chemically induced skin cancers. Nature Medicine, 2015, 21, 1514-1520.	15.2	93
17	The mutational signature profile of known and suspected human carcinogens in mice. Nature Genetics, 2020, 52, 1189-1197.	9.4	84
18	Multicolour lineage tracing reveals clonal dynamics of squamous carcinoma evolution from initiation to metastasis. Nature Cell Biology, 2018, 20, 699-709.	4.6	74

Allan Balmain

#	Article	IF	CITATIONS
19	The critical roles of somatic mutations and environmental tumor-promoting agents in cancer risk. Nature Genetics, 2020, 52, 1139-1143.	9.4	73
20	A functional switch from lung cancer resistance to susceptibility at the Pas1 locus in Kras2LA2 mice. Nature Genetics, 2006, 38, 926-930.	9.4	67
21	Mutational signatures in tumours induced by high and low energy radiation in Trp53 deficient mice. Nature Communications, 2020, 11, 394.	5.8	61
22	Inflammation and Hras signaling control epithelial–mesenchymal transition during skin tumor progression. Genes and Development, 2013, 27, 670-682.	2.7	50
23	Lgr6 is a stem cell marker in mouse skin squamous cell carcinoma. Nature Genetics, 2017, 49, 1624-1632.	9.4	47
24	Rewiring of human lung cell lineage and mitotic networks in lung adenocarcinomas. Nature Communications, 2013, 4, 1701.	5.8	42
25	Network analysis of skin tumor progression identifies a rewired genetic architecture affecting inflammation and tumor susceptibility. Genome Biology, 2011, 12, R5.	13.9	41
26	Identification of Hipk2 as an essential regulator of white fat development. Proceedings of the National Academy of Sciences of the United States of America, 2014, 111, 7373-7378.	3.3	38
27	Milestones in Skin Carcinogenesis: The Biology of Multistage Carcinogenesis. Journal of Investigative Dermatology, 2014, 134, E2-E7.	0.3	32
28	Modeling Cutaneous Squamous Carcinoma Development in the Mouse. Cold Spring Harbor Perspectives in Medicine, 2014, 4, a013623-a013623.	2.9	32
29	Chemical Carcinogenesis Models of Cancer: Back to the Future. Annual Review of Cancer Biology, 2017, 1, 295-312.	2.3	30
30	Targeting gene expression to tumor cells with loss of wild-type p53 function. Cancer Gene Therapy, 2000, 7, 4-12.	2.2	27
31	Genomic instability in radiation-induced mouse lymphoma from p53 heterozygous mice. Oncogene, 2005, 24, 7924-7934.	2.6	27
32	Chromosomal and genetic alterations of 7,12- Dimethylbenz[a]anthracene–induced melanoma from TP-ras transgenic mice. , 1997, 20, 78-87.		25
33	A Multilevel Model of Postmenopausal Breast Cancer Incidence. Cancer Epidemiology Biomarkers and Prevention, 2014, 23, 2078-2092.	1.1	25
34	Integration of multiple biological contexts reveals principles of synthetic lethality that affect reproducibility. Nature Communications, 2020, 11, 2375.	5.8	24
35	Targeting KRAS4A splicing through the RBM39/DCAF15 pathway inhibits cancer stem cells. Nature Communications, 2021, 12, 4288.	5.8	24
36	Gene Expression Architecture of Mouse Dorsal and Tail Skin Reveals Functional Differences in Inflammation and Cancer. Cell Reports, 2016, 16, 1153-1165.	2.9	20

Allan Balmain

#	Article	IF	CITATIONS
37	Genetic variation in the functional ENG allele inherited from the non-affected parent associates with presence of pulmonary arteriovenous malformation in hereditary hemorrhagic telangiectasia 1 (HHT1) and may influence expression of PTPN14. Frontiers in Genetics, 2015, 6, 67.	1.1	17
38	Sequential mutations in Notch1, Fbxw7, and Tp53 in radiation-induced mouse thymic lymphomas. Blood, 2012, 119, 805-809.	0.6	13
39	Panx3 links body mass index and tumorigenesis in a genetically heterogeneous mouse model of carcinogen-induced cancer. Genome Medicine, 2016, 8, 83.	3.6	13
40	The Trp53 delta proline (Trp53ΔP) mouse exhibits increased genome instability and susceptibility to radiation-induced, but not spontaneous, tumor development. Molecular Carcinogenesis, 2016, 55, 1387-1396.	1.3	5
41	Critical behavior of spatial networks as a model of paracrine signaling in tumorigenesis. Applied Network Science, 2019, 4, .	0.8	1